



**HAL**  
open science

## Measurement of $^{182,184,186}\text{W}$ ( $n, n' \gamma$ ) cross sections and what we can learn from it

G. Henning, Antoine Bacquias, Catalin Borcea, Mariam Boromiza, Roberto Capote, Philippe Dessagne, Jean-Claude Drohé, Marc Dupuis, Stephane Hilaire, Toshihiko Kawano, et al.

### ► To cite this version:

G. Henning, Antoine Bacquias, Catalin Borcea, Mariam Boromiza, Roberto Capote, et al.. Measurement of  $^{182,184,186}\text{W}$  ( $n, n' \gamma$ ) cross sections and what we can learn from it. PHYSOR 2020: Transition to a Scalable Nuclear Future, Mar 2020, Cambridge, United Kingdom. hal-02956052

**HAL Id: hal-02956052**

**<https://hal.science/hal-02956052>**

Submitted on 2 Oct 2020

**HAL** is a multi-disciplinary open access archive for the deposit and dissemination of scientific research documents, whether they are published or not. The documents may come from teaching and research institutions in France or abroad, or from public or private research centers.

L'archive ouverte pluridisciplinaire **HAL**, est destinée au dépôt et à la diffusion de documents scientifiques de niveau recherche, publiés ou non, émanant des établissements d'enseignement et de recherche français ou étrangers, des laboratoires publics ou privés.

## MEASUREMENT OF $^{182,184,186}\text{W}$ ( $\text{n}, \text{n}' \gamma$ ) CROSS SECTIONS AND WHAT WE CAN LEARN FROM IT.

**Greg Henning**

*Université de Strasbourg, CNRS, IPHC UMR 7178, F-67000 Strasbourg, France.*  
[ghenning@iphc.cnrs.fr](mailto:ghenning@iphc.cnrs.fr)

**Antoine Bacquias**<sup>1</sup>, **Catalin Borcea**<sup>2</sup>, **Mariam Boromiza**<sup>2</sup>, **Roberto Capote**<sup>3</sup>,  
**Philippe Dessagne**<sup>1</sup>, **Jean-Claude Drohé**<sup>4</sup>, **Marc Dupuis**<sup>5</sup>, **Stephane Hilaire**<sup>5</sup>,  
**Toshihiko Kawano**<sup>6</sup>, **Maëlle Kerveno**<sup>1</sup>, **Alexandru Negret**<sup>2</sup>, **Markus Nyman**<sup>4</sup>,  
**Adina Olacel**<sup>2</sup>, **Arjan Plompen**<sup>4</sup>, **Pascal Romain**<sup>5</sup>, **Gérard Rudolf**<sup>1</sup>, **Pol Scholtes**<sup>1</sup>.

- 1. Université de Strasbourg, CNRS, IPHC UMR 7178, F-67000 Strasbourg, France.*
- 2. Horia Hulubei National Institute for Physics and Nuclear Engineering, Bucharest-Magurele, Romania.*
- 3. IAEA, Nuclear Data Section, Vienna, Austria.*
- 4. European Commission, Joint Research Centre, B-2440 Geel, Belgium.*
- 5. CEA, DAM, DIF, F-91297 Arpajon, France.*
- 6. Theoretical Division, Los Alamos National Laboratory, Los Alamos, NM 87545, USA.*

### ABSTRACT

Today's development of nuclear installations rely on numerical simulation for which the main input are evaluated nuclear data. Inelastic neutron scattering ( $\text{n}, \text{xn}$ ) is a reaction of importance because it modifies the neutron population, the neutron energy distribution and may create new isotopes. The study of this reaction on tungsten isotopes is interesting because it is a common structural material. Additionally, tungsten isotopes are a good testing field for theories. The IPHC group started an experimental program with the GRAPhEME setup installed at the neutron beam facility GELINA to measure ( $\text{n}, \text{xn} \gamma$ ) reaction cross sections using prompt gamma spectroscopy and neutron energy determination by time-of-flight. The obtained experimental data provide constraints on nuclear reaction mechanisms models for  $^{182,184,186}\text{W}$ . Indeed, to reproduce correctly the experimental ( $\text{n}, \text{n}' \gamma$ ) cross-sections, the reaction codes must include accurate models of the reaction mechanism, nuclear de-excitation process and use correct nuclear structure information.

KEYWORDS: Neutron, nuclear reaction, reaction mechanism, neutron inelastic scattering, tungsten.

### 1. INTEREST OF ( $\text{n}, \text{n}'$ ) REACTION STUDY

Today most nuclear reactor developments are using evaluated databases for numerical simulations. These databases contain all necessary quantities for the simulations such as total and partial cross sections, angular distributions. However, these databases still contain large uncertainties and disagreements. To improve their level of precision, new measurements and theoretical developments are needed [1,2]. The ( $\text{n}, \text{xn}$ ) reactions are of particular interest as they modify the neutron spectrum, the neutron population, and produce radioactive species. To experimentally extract the total ( $\text{n}, \text{xn}$ ) cross section, the study of the ( $\text{n}, \text{xn} \gamma$ ) channels brings very strong constraints for the comparison with theoretical predictions as such calculation

requires a correct description of the reaction mechanism, the nuclear de-excitation process and the precise knowledge of the nuclear structure. The group at IPHC started a program to study the ( $n, xn \gamma$ ) reaction in 2005 and already worked on  $^{232}\text{Th}$ ,  $^{233,235,238}\text{U}$ ,  $^{\text{nat}},^{182,183,184,186}\text{W}$ ,  $^{\text{nat}}\text{Zr}$  and  $^{57}\text{Fe}$ . [3-5]. Tungsten is not an active element in nuclear reactors, but, with a high melting point (3422 °C), a strong mechanical resistance (Young's modulus: 600 GPa) [6], a low thermal expansion, low toxicity, and a high resistance to oxidation, it is used in many alloys. The interaction of neutrons with tungsten is therefore of importance for reactor physics, in particular for fusion reactors in which tungsten is one of the most exposed material to high energy neutrons [7]. As applications do not use isotopically pure material, one has to study all the natural isotopes:  $^{182}\text{W}$  (26.5 %),  $^{183}\text{W}$  (14.3 %),  $^{184}\text{W}$  (30.6 %),  $^{186}\text{W}$  (28.4 %) [8]. Only the even-even isotopes and inelastic ( $n, n' \gamma$ ) reaction will be discussed here. There are only a few measurements available today on these nuclides: some ( $n, 2n$ ) and ( $n, 3n$ ) cross section data exist, and a few ( $n, n'$ ) level populations cross sections have been measured [9–11], but ours is the only available data of that kind, and will provide a complete and constraining test to the predictability of models.

## 2. THE GRAPHEME EXPERIMENTAL SETUP

Measurements of ( $n, xn \gamma$ ) reaction cross sections using prompt  $\gamma$  ray spectroscopy and neutron energy determination by time of flight are performed at the neutron beam facility GELINA(EC/JRC Geel (Belgium) [12,13]. The GELINA accelerator provides a pulsed neutron beam with energies ranging from sub thermal to about 20 MeV, and a peak around 1-2 MeV for our experiment. The GRAPhEME setup is located 30 meters away from the neutron source and consists of a fission chamber to measure the incoming neutron flux and four HPGe detectors for the detection of  $\gamma$  rays. The whole setup is equipped with a digital acquisition [14]. The ratio of detected  $\gamma$  rays for a given transition to the number of neutrons (with the appropriate corrections factors and parameters) leads to the cross-section for the transition. A more detailed description of the experimental setup and method is given in references [15] and [16]. In order to produce the most complete data set, measurements were performed with  $^{\text{nat}}\text{W}$  and isotopically enriched  $^{182,184,186}\text{W}$  targets [17]. The data is analyzed using a Monte-Carlo (MC) method: the parameters involved in the ( $n, xn \gamma$ ) cross-sections are varied randomly within their estimated probability distributions. For each MC iteration, the cross section is calculated with a set of parameters. The results are combined to obtain the central value, standard deviation (i.e. uncertainty) and covariances [18].

## 3. RESULTS AND DISCUSSION

For each of the isotopes, about 20 gamma-ray production cross sections were extracted from the data sets. About ten transitions per isotope have been extracted from the natural tungsten data. The general cross section limit of detection is around 0.01 barn, depending on the data set, the transition energy and its possible internal conversion. The ( $n, 2n \gamma$ ) channel has not been studied, because long-lived isomers complicate the analysis. The cross check between the  $^{\text{nat}}\text{W}$  and isotopic targets data allowed us to resolve a quantity of matter in the natural target [17]. The experimental data are compared to calculations by the codes TALYS, EMPIRE and CoH3. The TALYS-1.73 calculations [19,20], used a fine tuned optical potential with coupled channels optimized for deformed nuclei such as tungsten. The nuclear structure considered contained 30 discrete levels. Finally, the M1 low energy scissor mode was included in the  $\gamma$ -strength function. The EMPIRE calculations [21,22] were performed using the model parameters described in references [23,24]. The parameters were not optimized to describe the ( $n, xn \gamma$ ) transitions and further work is needed to get a more reliable output. For CoH3 [25], a coupled-channels neutron optical potential was used, with nuclear deformation parameters taken from Finite Range Droplet Model. The code uses a Gilbert-Cameron level density and pre-equilibrium spin distributions where obtained using Feshbach-

Kerman-Koonin (FKK) approach. The calculation used 70 discrete levels with levels included inside the continuum. See references [26] and [27] for more details on CoH3 calculations.

### 3.1. Ground state rotational band transitions

The structure of the three isotopes  $^{182,184,186}\text{W}$  is very similar, with a strong rotor-like behavior. The *yrast* states form a rotational band built on the  $0^+$  ground state. The  $2^+$  to ground state transition is expected to be the one of the most intense in the level scheme as up to 90 % of the decay paths lead to the  $2_{\text{gsb}}^+$  state (*gsb* stands for “ground state band”). It is therefore of particular importance to characterize it properly and reproduce it in the calculations. Figure 1 gives the cross sections for the  $2^+_{\text{gsb}}$  to g.s.  $\gamma$ -rays in the three isotopes. In the plots (and subsequently for the other transitions), the cross section error bars represent one standard deviation of a Gaussian distribution. The neutron energy error bars represent the range in neutron energy for which the average cross section is given by the point. Some overlap in x-error bars may occur, reflecting the uncertainty in neutron energy selection. For  $^{182}\text{W}$  transitions studied in the  $^{\text{nat}}\text{W}$  target, some  $(n, 2n \gamma)$  reactions on the  $^{183}\text{W}$  present in the target lead to a contamination of the  $^{182}\text{W}(n, n' \gamma)$  cross section above  $S_n$ . For the  $2^+ \rightarrow \text{g.s.}$  (and after for the  $4^+ \rightarrow 2^+$ ) transitions, a correction was performed by removing the  $^{183}\text{W}(n, 2n \gamma)$  contribution calculated with TALYS-1.7 with default parameters to the experimental data. Some magnitude variation between the different isotopes is observed and reflect the change in internal conversion (IC) rather than the transition intensity.

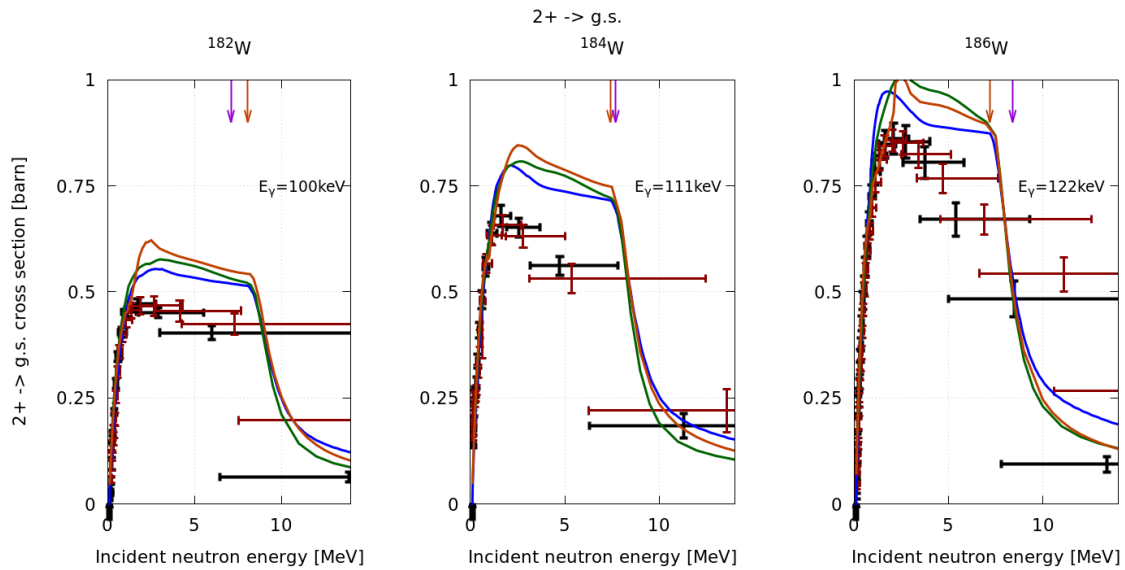


**Figure 1.**  $(n, n' \gamma)$  cross sections measured with GRAPhEME for the isotopes  $^{182}\text{W}$  (left),  $^{184}\text{W}$  (center),  $^{186}\text{W}$  (right), for the first excited state ( $2^+_{\text{gsb}}$ ) to the ground state transition. The data from isotopic targets are represented with black crosses, the data from the  $^{\text{nat}}\text{W}$  target in red (corrected for  $^{183}\text{W}(n, 2n \gamma)$  contamination for  $^{182}\text{W}$ ). It is compared to TALYS-1.73 (blue line), EMPIRE (orange line) and CoH3 (green line) calculations. The excitation energy of the decaying level is marked with the black up-pointing arrow on the bottom axis. The neutron separation energy  $S_n$  and proton separation energy  $S_p$  are marked with the orange and purple down-pointing arrows at the top, respectively.

The reaction codes reproduce correctly the shape and amplitude of the experimental cross section up to about neutron energy of 1 MeV, but above the magnitude is not correct. Furthermore, the calculations

present a kind of plateau of the cross section from the peak to 8 MeV where there is a sharp drop in the experimental data. We investigated if this could be an effect of large uncertainty in the HPGe detectors timing due to non-linear response for low energy  $\gamma$  rays. However, we could not conclude that it could explain this discrepancy. The impact of high energy discrete states decaying directly to the ground state (and thus depleting the cross section of the  $2^+ \rightarrow \text{g.s.}$  transition) that would be missing in the known nuclear structure was also looked into. But the impact of such a state and transition would be too large for it to be unobserved. We will notice below that the other transitions in the ground state band (in particular  $4^+ \rightarrow 2^+$ ) present an excess of cross section in the calculations at this neutron energy range. One can therefore speculate that the overestimated cross sections from the models within the ground state band are (at least partly) responsible for the behavior seen in the  $2^+ \rightarrow \text{g.s.}$  transition. Figure 2 shows the  $4^+ \rightarrow 2^+$  transitions. As mentioned above, the calculations show an excess of cross section in the 2 to 9 MeV range, which could explain the significant slope difference between experimental and calculated values in the  $2^+ \rightarrow \text{g.s.}$  transition. Figure 3 shows the transitions for  $6^+ \rightarrow 4^+$ . The  $8^+ \rightarrow 6^+$  (not represented here) transition is very weak and barely observable for  $^{184}\text{W}$  and  $^{186}\text{W}$  because the  $8^+$  (and in general high spin states) state(s) is weakly populated in inelastic neutron scattering. The TALYS and EMPIRE calculations overestimate the cross section by a factor of 2 for the  $4^+ \rightarrow 2^+$  and up to 6 fold for the  $8^+ \rightarrow 6^+$  transition. This is not observed in the CoH3 calculations. We attribute this discrepancy between the data and TALYS, EMPIRE calculations to the effect of the spin distribution in the entrance channel, computed using phenomenological models. Indeed, the *classic* “exciton” model predict and average spin of the residual nucleus around 8-10  $\hbar$  while microscopic QRPA calculations have this value down to 3-4  $\hbar$  [28]. The exact same behavior has been observed in  $^{238}\text{U}$  [4]. Additionally, the use of level densities to describe the high lying states may be worse than the explicit use of discrete levels in the continuum as done by CoH3.

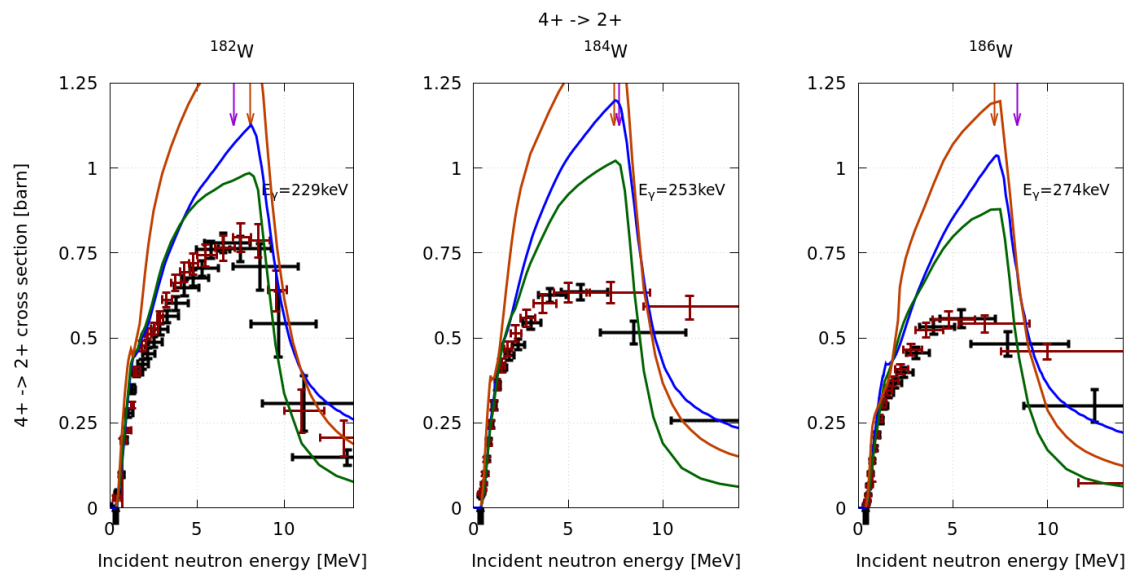


Figure 2. Same as figure 1, for the  $4^+$  to  $2^+$  transition in the ground state band.

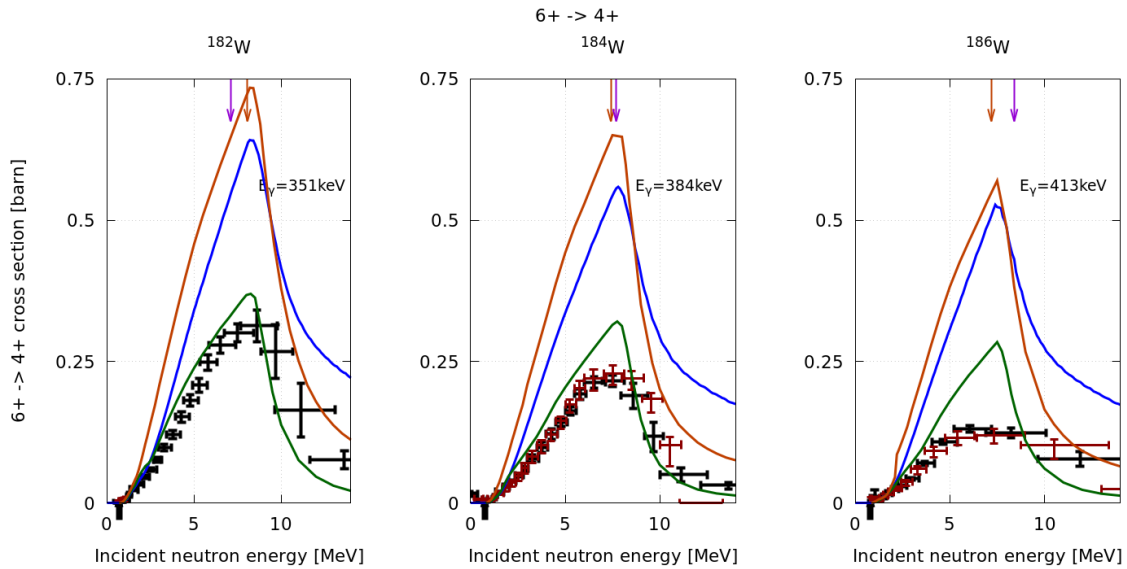


Figure 3. Same as figure 1, for the  $6^+$  to  $4^+$  transition in the ground state band. No data for  $^{182}\text{W}$  could be extracted from the  $^{\text{nat}}\text{W}$  dataset.

### 3.2. Transitions in the beta band

The so-called “beta” band is a rotor like band built on an excited  $0^+$  state, with a moment of inertia just slightly larger than the one of the ground state rotational (*yrast*) band. The band head state  $0^+$  decays by emitting a  $\gamma$  ray to the  $2^+$  state in the ground state band. These transitions are experimentally measured with varying sensitivity depending on the isotope. Figure 4 shows the cross section plots. The models reproduce the experimental values well for  $^{182}\text{W}$  and  $^{184}\text{W}$ . TALYS and EMPIRE agree with the data for the heaviest isotope but CoH3 present an excess of cross section for neutron energies above 2 MeV. This could be linked to incorrect structure information.

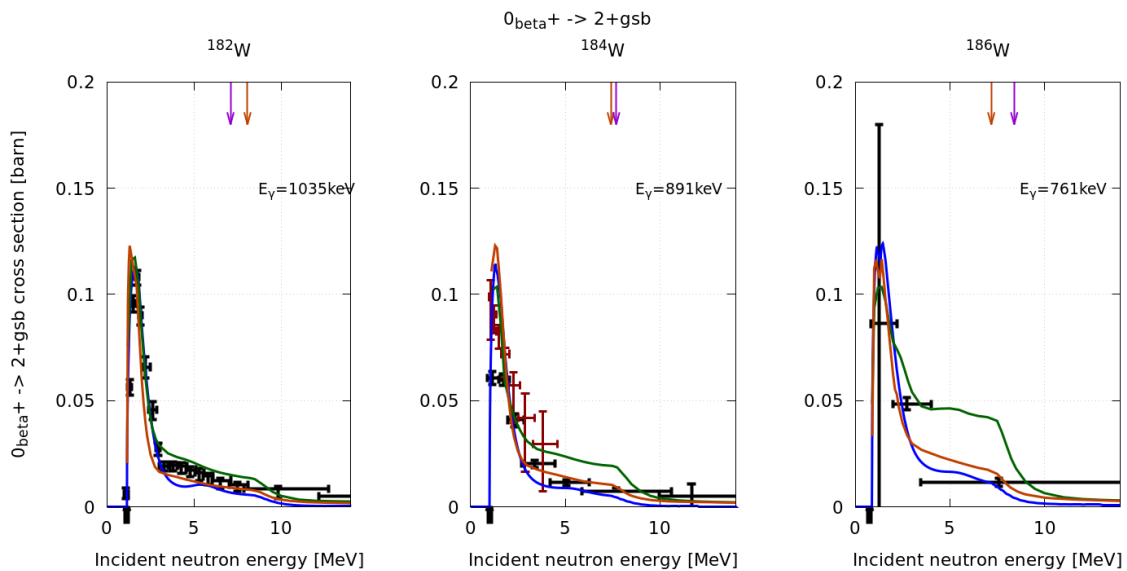


Figure 4. Same as figure 1, for the  $0^+_{\text{beta}}$  to  $2^+_{\text{gsb}}$  transition. Data could be extracted from the  $^{\text{nat}}\text{W}$  dataset only for  $^{184}\text{W}$ .

The next state in the band:  $2^+$ , decays to the  $0^+$ ,  $2^+$ ,  $4^+$  states in the ground state band. Across these three transitions, TALYS does the best job at reproducing the experimental data. In particular for the  $2_{\text{beta}^+}$  to g.s. transitions (figure 5). However, for the  $2_{\text{beta}^+}$  to  $2_{\text{gsb}^+}$  and  $2_{\text{beta}^+}$  to  $4_{\text{gsb}^+}$  (figures 6 and 7), even if the calculations are mostly in line with experimental data for  $^{182}\text{W}$  and  $^{186}\text{W}$ , it is not the case for  $^{184}\text{W}$  for which TALYS and CoH3 (no EMPIRE calculations available for  $^{184,186}\text{W}$ ) overestimate the cross section by a factor of about 2. One can speculate that it is linked to an issue in the level structure and the branching ratios of the  $\gamma$  rays or a possible missing transition in the structure database.

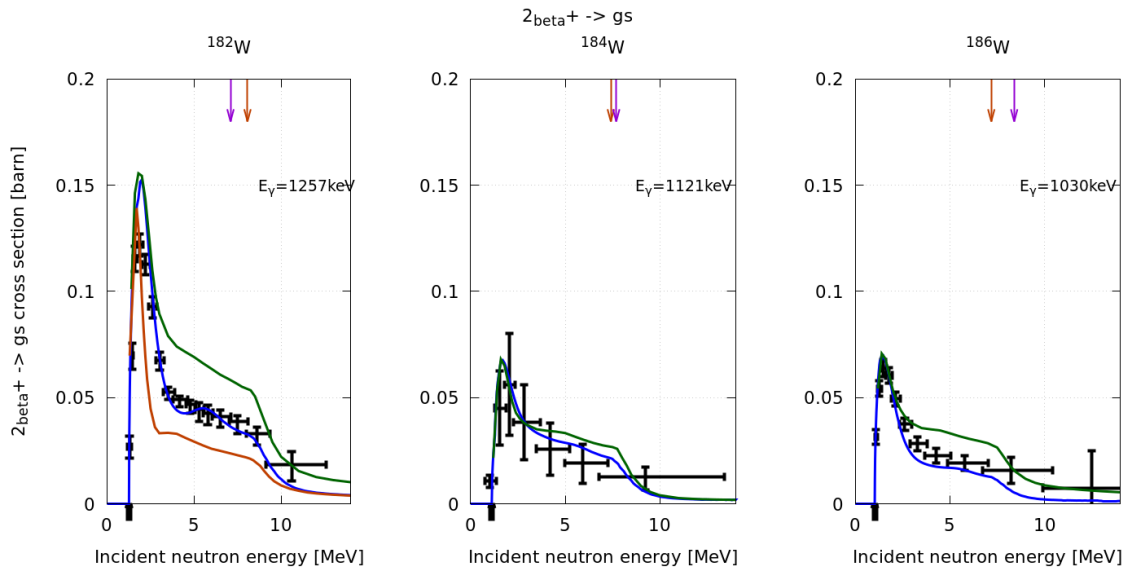


Figure 5. Same as figure 1, for the  $2^+_{\text{beta}}$  to g.s. . No data could be extracted from the  $^{\text{nat}}\text{W}$  dataset.

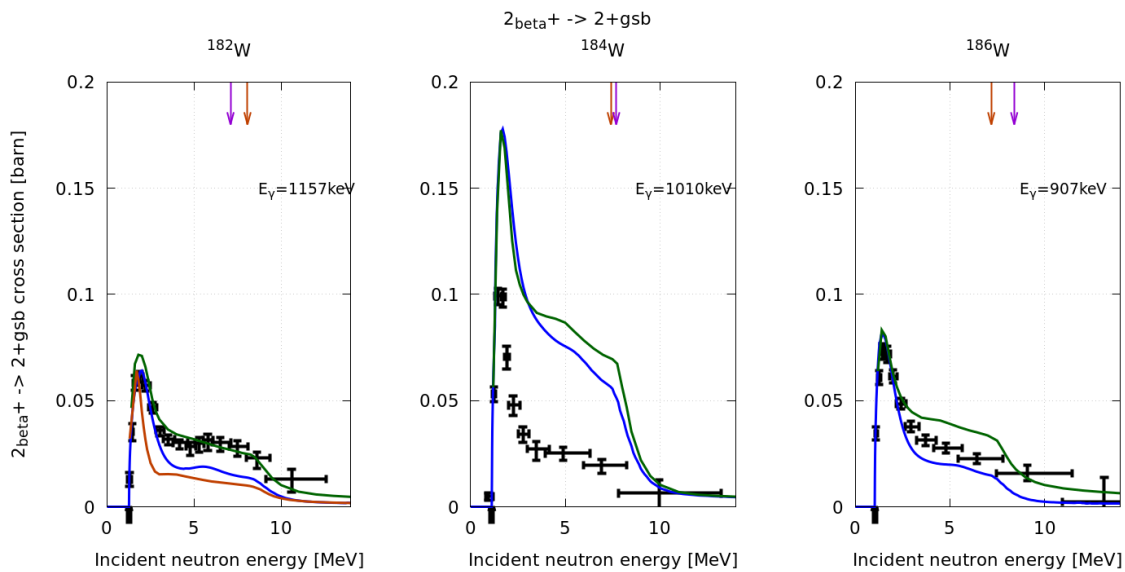
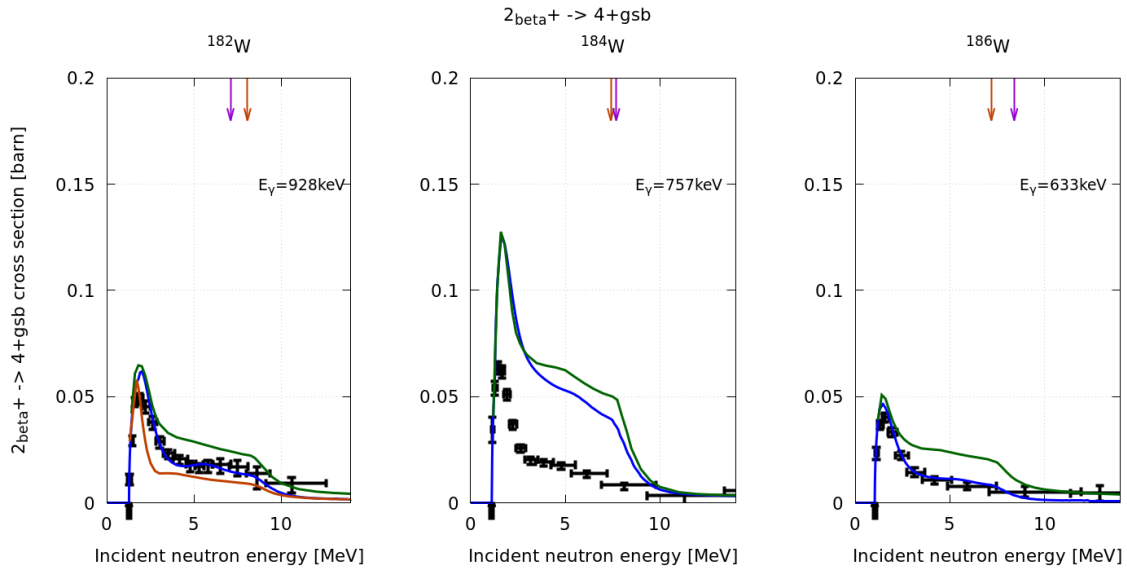


Figure 6. Same as figure 1, for the  $2^+_{\text{beta}}$  to  $2^+_{\text{gsb}}$  transition. No data could be extracted from the  $^{\text{nat}}\text{W}$  dataset.



**Figure 7. Same as figure 1, for the  $2^+_{\text{beta}}$  to  $4^+_{\text{gs}}$  transition. No data could be extracted from the  $^{nat}\text{W}$  dataset.**

#### 4. CONCLUSIONS

We presented the first ever data set of  $\gamma$ -ray cross-sections for  $^{182,184,186}\text{W}(n, n' \gamma)$ . These data were measured using both natural (mixed isotopes) and isotopically pure targets, in order to perform cross checks between the data sets. The obtained cross-sections present a varying degree of agreement with results from calculations. From the comparison, we could conclude that better entrance channel calculations such as QRPA and a more accurate description of the level structure at the continuum limit can help resolve discrepancies in the high spin region. There are still significant disagreements between experimental values and calculations. From past results on other nuclei, we are confident that they can be solved by fixing level structure information: indeed, branching ratios, missing transitions and intensity have been shown to play a significant role in the model predictions.

#### ACKNOWLEDGMENTS

The authors thank the team at the GELINA facility and IPHC for their support. This work was funded in part by NEEDS, PACEN/GEDEPEON, and by the European Commission within the Sixth Framework Program through I3-EFNUDAT (EURATOM contract No. 036434) and NUDAME (Contract FP6-516487), and within the Seventh Framework Program through EUFRAT (EURATOM contract No. FP7-211499), through ANDES (EURATOM contract No. FP7-249671).

## REFERENCES

1. R. Jacqmin, M. Salvatores, "Uncertainty and target accuracy assessment for innovative systems using recent covariance data evaluations", NEA/WPEC(NEA/OECD, 2008), ISBN: 9789264990531
2. G. Aliberti, et al. "Annals of Nuclear Energy" 33, 700 (2006)
3. M. Kerveno, et al. "(n,xn gamma) reaction cross section measurements for (n,xn) reaction studies," EPJ Web of Conferences, vol. 42, p. 01005, 2013.
4. M. Kerveno, et al., "From gamma emissions to (n,xn) cross sections of interest : the role of GAINS and GRAPhEME in nuclear reaction modeling." Eur. Phys. J. A, 51 12 (2015) 167
5. Eliot Party, et al. « Neutron inelastic scattering of  $^{232}\text{Th}$ : measurements and beyond". EPJ Web of Conferences, EDP Sciences, 2019, 211, pp.03005.
6. W. Haynes, "CRC Handbook of Chemistry and Physics." Taylor & Francis, 2012.
7. M. Gilbert, S. Dudarev, S. Zheng, L. Packer, and J.-C. Sublet, "An integrated model for materials in a fusion power plant: transmutation, gas production, and helium embrittlement under neutron irradiation," Nuclear Fusion, vol. 52, no. 8, p. 083019, 2012.
8. J. R. de Laeter, et al. "Atomic weights of the elements. Review 2000" (IUPAC Technical report), vol. 75, 2009.
9. IAEA nuclear data services website. <https://www-nds.iaea.org/exfor/>
10. D. Lister, A. B. Smith, and C. Dunford, "Fast-neutron scattering from the 182, 184, and 186 isotopes of tungsten," Phys. Rev., vol. 162, pp. 1077-1087, Oct 1967.
11. P. T. Guenther, A. B. Smith, and J. F. Whalen, "Fast-neutron total and scattering cross sections of  $^{182}\text{W}$ ,  $^{184}\text{W}$ , and  $^{186}\text{W}$ ," Phys. Rev. C, vol. 26, pp. 2433-2446, Dec 1982.
12. D. Tronc, J. Salomé, and K. Bockhoff, "A new pulse compression system for intense relativistic electron beams," Nuclear Instruments and Methods in Physics Research Section A: Accelerators, Spectrometers, Detectors and Associated Equipment, vol. 228, no. 2-3, pp. 217 - 227, 1985.
13. D. Ene, et al., "Global characterisation of the Gelina facility for high-resolution neutron time-of-flight measurements by monte carlo simulations," Nuclear Instruments and Methods in Physics Research Section A: Accelerators, Spectrometers, Detectors and Associated Equipment, vol. 618, no. 1-3, pp. 54 - 68, 2010
14. L. Arnold, et al. "Tnt digital pulse processor," IEEE Computer Society, 2005, pp. 265–269.
15. G. Henning et al., "GRAPhEME: A setup to measure (n, xn  $\gamma$ ) reaction cross sections," 2015 4th International Conference on Advancements in Nuclear Instrumentation Measurement Methods and their Applications (ANIMMA), Lisbon, 2015, pp. 1-9.
16. J. Thiry, "Measurement of (n,xn gamma) Reaction Cross Sections of Interest for the Generation IV Reactors". PhD thesis, Université de Strasbourg, 2010.
17. Greg Henning et al. "Measurement of (n, xn gamma) reaction cross sections in W isotopes". EPJ Web of Conferences 146, 11016 (2017)
18. M. Kerveno et al., "How to produce accurate inelastic cross sections from an indirect measurement method?" EPJ Nuclear Sci. Technol. 4 23 (2018)
19. A. Koenig, S. Hilaire, M. Duijvestijn, "TALYS-1.0" International Conference on Nuclear Data for Science and Technology (2007), EDP Sciences, 2008, pp. 211-214, <http://www.talys.eu/>
20. P. Romain, private communication
21. M. Herman, R. Capote, et al., Nucl. Data Sheets 108, 2655 (2007)
22. R. Capote, private communication
23. A. Trkov, R. Capote, I. Kodeli, L. Leal, Nuclear Data Sheets 109, 2905 (2008)
24. A. Trkov, R. Capote, et al. Nuclear Data Sheets 112, 3098 (2011)
25. T. Kawano, private communication
26. T. Kawano, R. Capote, S. Hilaire, P. Chau Huu-Tai, Phys. Rev. C 94, 014612 (2016)
27. T. Kawano, et al., Journal of Nuclear Science and Technology 47, 462 (2010)
28. M. Dupuis, et al. "Microscopic modeling of direct pre-equilibrium emission from neutron induced reactions on even and odd actinides.," EPJ Web Conf. 146 12002 (2017)